



Published in final edited form as:

*J Mol Biol.* 2013 January 09; 425(1): 82–93. doi:10.1016/j.jmb.2012.11.008.

## An insertion in the catalytic trigger loop gates the secondary channel of RNA polymerase

Ran Furman<sup>1</sup>, Oleg V. Tsodikov<sup>2</sup>, Yuri I. Wolf<sup>3</sup>, and Irina Artsimovitch<sup>1,\*</sup>

<sup>1</sup>Department of Microbiology and The Center for RNA Biology, The Ohio State University, Columbus, OH, USA

<sup>2</sup>Department of Medicinal Chemistry, College of Pharmacy, University of Michigan, Ann Arbor, MI, USA

<sup>3</sup>National Center for Biotechnology Information, National Library of Medicine, National Institutes of Health, Bethesda, MD, USA

### Abstract

*Escherichia coli* DksA and GreB bind to RNA polymerase, reaching inside the secondary channel, with similar affinities but have different cellular functions. DksA destabilizes promoter complexes whereas GreB facilitates RNA cleavage in arrested elongation complexes. Although the less abundant GreB may not interfere with DksA regulation during initiation, reports that DksA acts during elongation and termination suggest that it may exclude GreB from arrested complexes, potentially triggering genome instability. Here we show that GreB does not compete with DksA during termination whereas DksA, even when present in several hundred-fold molar excess, does not inhibit GreB-mediated cleavage of the nascent RNA. Our findings that DksA does not bind to backtracked or active elongation complexes provide an explanation for the lack of DksA activity on most elongation complexes that we reported previously, raising a question of what makes a transcription complex susceptible to DksA. Structural modeling suggests that i6, an insertion in the catalytic trigger loop, hinders DksA access into the channel, restricting DksA action to a subset of transcription complexes. In support of this hypothesis, we demonstrate that deletion of i6 permits DksA binding to elongation complexes and that the distribution of DksA and i6 in bacterial genomes is strongly concordant. We hypothesize that DksA binds to transcription complexes in which i6 becomes mobile, for example as a consequence of weakened RNA polymerase interactions with the downstream duplex DNA.

### Keywords

DksA; Gre; RNA polymerase; secondary channel; trigger loop

---

\*corresponding author: artsimovitch.1@osu.edu phone 614-292-6777.

### Supplementary Data

Supplementary data associated with this article can be found in the online version, at ....

## Introduction

In multi-subunit RNA polymerases (RNAPs), the active site is accessible from the outside via the secondary channel (SC; also called the pore in pol II). Regulatory proteins that bind within this channel control transcription through altering properties of RNAP. These proteins consist of an extended domain, which binds within the SC, and a globular domain, which binds to the RNAP surface outside of the SC. The sequences and even structures of these proteins can be very different, and so are their effects on transcription. In *Escherichia coli*, five different SC regulators, DksA, GreA, GreB, Rnk and TraR<sup>1; 2; 3; 4; 5</sup>, have been characterized and other candidates are suggested by genome analysis.

*E. coli* GreA, GreB and DksA share the basic two-domain architecture – an extended coiled-coil (CC) domain and a globular domain (Fig. 1a), but play very different roles in the cell. DksA functions predominantly during initiation to tune rRNA synthesis to cellular cues<sup>6</sup>. Gre factors rescue elongation complexes (ECs) that become arrested when RNAP makes an error or runs into a roadblock<sup>7</sup>. However, the effects of GreB and DksA are not limited to a single step in the transcription cycle; recent studies demonstrate that both factors affect initiation and elongation<sup>8; 9</sup> and could play partially overlapping roles in DNA repair<sup>10; 11; 12</sup>. GreB and DksA are thought to interact with the same RNAP region, the  $\beta'$  rim helices (RH) domain<sup>5; 8</sup>, and bind to free RNAP with similar affinities<sup>9</sup>, but do not interact with nucleic acids. It is therefore unclear how they recognize their cellular targets and avoid competition with each other.

GreB and DksA are present at constant levels in the cell, but DksA is ten times more abundant<sup>9</sup>. Thus, GreB would not be expected to interfere with DksA during transcription initiation but, when overexpressed, can substitute for some (negative control of rRNA synthesis) but not other (activation of aminoacid biosynthetic genes) activities of DksA<sup>9</sup>. Conversely, since DksA affects RNA chain elongation but lacks the ability of GreB to enhance the nascent RNA cleavage<sup>8</sup>, DksA could, in principle, inhibit GreB function by blocking GreB binding to arrested ECs. This hypothetical competition would be avoided if DksA and GreB recognized different subsets of ECs; indeed, GreB action appears to be restricted to ECs in which the  $\beta'$  trigger loop (TL) is unfolded<sup>7</sup>.

We recently reported that *E. coli* DksA, and especially its hyperactive variant DksAN88I that increases affinity for free RNAP<sup>13</sup>, decreased the rate of elongation and increased termination<sup>8</sup>. However, we could not detect any DksA effect on isolated ECs, leaving an identity of its target unknown. Interestingly, DksA activity during elongation was strongly augmented by a deletion of a species-specific insertion in the TL (called *i6* or SI3; *E. coli*  $\beta'$  residues 943–1130), in sharp contrast to the resistance of the *i6* RNAP to GreB-mediated cleavage<sup>14</sup>. We hypothesized that DksA and GreB bind to different subsets of ECs, and that *i6* plays a key role in this discrimination, either directly, by modulating the transcription factor binding, or indirectly, through a coupled conformational change in the TL.

Here, we present evidence for a direct effect of *i6* on DksA recruitment. Structural modeling suggests a mechanism where *i6* physically hinders DksA access into the channel, and we show that the deletion of *i6* increases DksA affinity for the ECs but not for core RNAP.

Consistent with the key role of i6 in selective DksA recruitment, we find that i6 is present in every bacterial genome that has DksA. Based on these observations, we hypothesize that the DksA effect on elongation and termination reported by us previously<sup>8</sup> is mediated through targeting of a transient intermediate in which the i6 position is altered, e.g., due to changes in RNAP/DNA interactions or conformational transitions of the TL.

## Results

### DksA and GreB bind to the same target on RNAP

*E. coli* DksA and GreB have no sequence homology but share strikingly similar architecture (Fig. 1a) and interact with the same sites on RNAP. Structurally similar CC domains bind inside the SC, positioning the two acidic residues near the RNAP active site; •OH radicals generated by the Fe<sup>2+</sup> ion bound in place of the catalytic Mg<sup>2+</sup> ion induce cleavage at the tip of the CC of GreB and DksA (Fig. 1b). Structurally different globular domains are thought to interact with the β' RH domain that lies at the entrance into the SC. For *E. coli* GreB, this mode of binding is supported by extensive biochemical data and structural modeling<sup>3; 5; 15; 16</sup>, as well as the structure of its *Thermus thermophilus* homolog Gfh1 bound to EC<sup>17</sup>. Partially overlapping effects of DksA and GreB on initiation<sup>9</sup>, inhibition of their binding to RNAP by substitutions of Leu672 and Val673 at the RH tip<sup>5; 8</sup>, and a report that a single residue substitution at the CC tip of GreA is sufficient to confer DksA-specific regulatory effects at rRNA and amino acid biosynthesis promoters<sup>18</sup> argue for the common binding site.

Consistently, GreB efficiently competed with DksA for binding to the wild-type (WT) RNAP, whereas the deletion of the entire i6 domain reduced the competition between the two factors (Fig. 1b). This observation is consistent with previous reports that i6 RNAP is insensitive to GreB<sup>14</sup> but hypersensitive to DksA<sup>8</sup>. NusG, which binds to a distant β' clamp helices domain, had no effect on DksA binding. Similar results were obtained with GreA (Supplementary Fig. 1).

### DksA and GreB do not functionally compete during elongation

GreB does not affect elongation or termination, but reactivates arrested, backtracked ECs through cleavage of the nascent RNA<sup>3</sup>. In contrast, DksA inhibits elongation and increases termination but has no effect on RNA cleavage<sup>8</sup>. Exclusion of GreB by the more abundant DksA could lead to increased RNAP stalling *in vivo*. To test whether GreB and DksA would functionally compete *in vitro*, we used RNA cleavage and termination assays.

RNAP possesses intrinsic hydrolytic activity which allows successive removal of the 3' RNA fragments in a stalled EC; this activity is dramatically enhanced by GreB<sup>3</sup>. We used halted A26 ECs which are sensitive to RNA hydrolysis (Fig. 2a) to test DksA effect on this reaction. In this study and in our previous work, we took advantage of a “hyperactive” DksA<sup>N88I</sup> variant<sup>13</sup> to increase DksA occupancy on RNAP. The available evidence indicates that the only effect of this substitution is to increase DksA affinity for RNAP<sup>8; 13</sup>; nonetheless, to exclude potential artifacts, we repeated all the key experiments with a higher concentrations of WT DksA. RNAP alone cleaved the nascent RNA very slowly, whereas

the addition of GreB led to rapid shortening of RNA; note that the cleavage products in the absence and in the presence of GreB were different. DksA<sup>N88I</sup> did not induce RNA cleavage and did not interfere with the stimulatory effect of GreB when present at a 100-fold molar excess (Fig. 2a). Similarly, WT DksA, which binds to RNAP with a five-fold lower affinity than DksA<sup>N88I</sup> does, failed to block GreB-enhanced cleavage when present at 300-fold excess (Supplementary Fig. 2). GreB, when present in a 10-fold molar excess, did not affect termination at *rmb* T1 and did not interfere with DksA effect therein (Fig. 2b).

We conclude that, although GreB and DksA have similar affinities for core RNAP<sup>9</sup>, they recognize different ECs. GreB, which targets backtracked ECs<sup>7</sup>, bound to free core RNAP and backtracked EC much better than to active ECs (Supplementary Fig. 3). In contrast, DksA interactions with both backtracked and active EC were much weaker than with the core enzyme (Fig. 2c), suggesting that DksA may be excluded from most ECs. In the absence of a known mechanistic target for DksA, we turned to structural modeling for an answer.

### A model for DksA-EC suggests restricted access to the SC

The published model of an RNAP-DksA complex, which is comprised of *T. thermophilus* RNAP and *E. coli* DksA<sup>4</sup>, is consistent with some experimental data, such as competition with GreB for binding to RNAP, but it does not explain other results, such as the effects of changes at the RH tip on DksA binding<sup>8</sup>. This model was built on the assumption that in the DksA-RH complex the interactions between the CC domain of DksA and RH closely resemble the packing contacts between the CC domains of two DksA molecules in the crystal.

Using a recently published hybrid EM/X-ray model of an *E. coli* EC<sup>19</sup>, we constructed a model of DksA bound to EC (Fig. 3); see Methods for details. This model explains the observed effects of DksA Asn88Ile<sup>13</sup> and RH Leu672/Val673 substitutions<sup>8</sup> on DksA/RNAP interactions and reveals two minor clashes between DksA and RNAP. The N-terminal helix of DksA (residues 12–18) clashes with RH; this clash can be removed by repositioning of the N-terminus, which may be flexible. We also observe a clash between the base of the DksA CC domain and i6, which could in principle be removed by a pivoting movement of i6 relative to the body of RNAP. This clash is consistent with the stimulation of DksA activity by the i6 deletion<sup>8</sup> and may also explain why DksA binds with high affinity to free RNAP but not to open complexes<sup>20</sup> or most ECs where the i6 position may be constrained (see Discussion).

We do not have experimental evidence for conformational changes in RNAP upon DksA binding but we note that a small shift in i6 would be sufficient to accommodate DksA in the SC. In contrast, binding of other SC regulators may be accompanied by dramatic structural changes, e.g., “ratcheting” observed with Gfh1<sup>17</sup>. A model of GreB bound to the *E. coli* EC suggests that GreB would severely clash with i6 (Supplementary Fig. 4), unless i6 undergoes a large-scale movement, for example, upon unfolding of the TL<sup>7</sup>. However, dramatic changes in the GreB-bound EC remain to be demonstrated, whereas the inhibition of RNA chain elongation by a cleavage-deficient GreB variant<sup>3</sup> and the ability of GreB to bind to the

active EC (Supplementary Fig. 3) suggest that such changes may not be absolutely necessary.

A potential limitation of our model lies in the assumption that DksA is rigid, whereas even minor rotations and translations would affect individual contacts between RNAP and DksA. Therefore, this model is cannot predict specific interactions between the two proteins. Consequently, in our analysis we use gross features of the model, the relative dispositions of the contacting regions of DksA and RNAP.

We next tested several predictions of this model using deletion variants of DksA and RNAP. First, since  $\beta'$  RH interacts with the C-terminal helix of DksA, deletion of this helix would be expected to compromise DksA binding. We found that deletions of five and ten C-terminal residues in DksA compromised its effect on transcription (Fig. 4a) and the deletion variants failed to compete with the WT DksA for binding to core RNAP (Supplementary Fig. 5). Although we cannot exclude a possibility that these truncations may alter DksA structure, observations that (i) this region makes no contacts to the rest of the protein<sup>4</sup>; (ii) the truncated proteins exhibit similar to the WT DksA expression levels, solubility, chromatographic behavior, and differential scanning fluorescence profiles (RF and IA, unpublished data); and (iii) a DksA variant containing a stop codon at Glu146 (a 6-residue deletion) is stable *in vivo*<sup>21</sup> argue against dramatic structural changes.

Second, since the N-terminal helix of DksA clashes with RH, removing this clash may favor DksA entry into the SC. Consistently, a deletion of N-terminal 18 residues potentiated DksA effect on initiation (Supplementary Fig. 6) and termination (Fig. 4a). Interestingly, a substitution of Leu15 for Phe increased DksA affinity for RNAP<sup>13</sup>; we hypothesize that this substitution destabilizes interactions between the N- and C-terminal parts of DksA, thereby relieving the clash between N-terminal helix and RH.

Third, since i6 movements are not constrained in the absence of the nucleic acids, DksA should bind to core RNAP with higher affinity than to ECs. Using Fe-mediated cleavage assay<sup>20</sup>, we found that DksA affinity for the active EC was reduced 14 fold (Fig. 4c). DksA affinity for the backtracked EC could not be measured accurately at attainable EC-2 concentrations; we estimate at least 20-fold reduction in affinity. The SC regulators may bind to RNAP in two steps, first docking on the RH and then entering the SC *ad hoc*<sup>22</sup>. Similar K<sub>d</sub> values obtained by Fe-mediated •OH cleavage assay, which detects only the second step, and fluorescence anisotropy<sup>8</sup>, which measures total binding, are consistent with a single binding mode for DksA, at least with the core RNAP.

The extent of DksA cleavage was significantly reduced in the EC as compared to the core enzyme. Similar effects were observed by Gourse and colleagues in DksA-RPo complex<sup>20</sup> and with DksA variants<sup>18</sup>. These authors concluded that the efficiency of cleavage by •OH generated at the RNAP active site is an indicator of the local conformation of the CC tip region, rather than a quantitative measure of DksA affinity, the lifetime of the DksA-RNAP complex, or its functional state. The reduced DksA cleavage in the EC may be due to an increased distance between the CC tip and the active site or to the quenching action of the TL that may become folded upon interactions with DksA (see Discussion).

Fourth, removal of i6 would allow unimpeded DksA access into the SC in the EC. Indeed, an apparent affinity of WT DksA to the EC formed with the i6 RNAP was more than five-fold higher than to the WT EC. In contrast, in the absence of a nucleic acid scaffold DksA interacted with both the WT and the i6 RNAPs similarly (Fig. 4b, c), consistent with i6 flexibility in core RNAP.

Finally, we reasoned that the deletion of the jaw, which interacts with i6 and likely with the downstream DNA<sup>23</sup> and reduces lifetimes of open promoter complexes similarly to i6<sup>24;25</sup>, may also favor the action of DksA. We found that a deletion in the jaw ( $\beta'$  residues 1149–1190) makes RNAP hypersensitive to DksA (Fig. 4a and Supplementary Fig. 6) and allows DksA binding to the EC formed by the jaw RNAP, although the effect was less dramatic than that conferred by the deletion of i6 (Fig. 4c). In combination, these results support the proposed mode of DksA interactions with the EC (Fig. 3).

### Genome analysis reveals concordant distribution of i6 and DksA

Our model suggests that the  $\beta'$  i6 domain restricts DksA entry into the SC to ensure that DksA does not bind to EC indiscriminately. If this hypothetical role of i6 were important, i6 would be expected to be present in genomes that encode DksA. To ask whether this were true, we analyzed DksA and i6 distribution in microbial genomes. To reduce the effects of the sampling bias, we carried out this analysis using 572 genomes representing their genera from the set of 1515 completely sequenced genomes (see Supplementary Data for details).

We first needed to define i6 and DksA. The i6 domain is located at positions 943–1130 of *E. coli*  $\beta'$  and is flanked by relatively conserved segments of TL, but is variable among different species (Supplementary Fig. 7). Here, we labeled all proteins with insertions exceeding 60 residues at this position as i6 positive.

DksA belongs to a diverse group of DksA/TraR regulators that constitute COG1734<sup>26</sup>. *E. coli* DksA has two characteristic features, a Cys4 Zn finger proposed to determine the orientation of the two domains<sup>4</sup>, and a long CC with two Asp residues at its tip (Fig. 1). Interestingly, neither the Zn finger nor the CC domain is indispensable. *Pseudomonas aeruginosa* DksA2 has a full-length CC but carries substitutions in the Zn finger (Fig. 5a) which eliminate zinc binding<sup>27</sup> but do not dramatically alter the structure (RF et al., in preparation), whereas *E. coli* TraR contains a Cys4 Zn finger but lacks the N-terminal helix of the CC motif. Both proteins act similarly to *E. coli* DksA *in vitro* and partially compensate for its absence *in vivo*<sup>1;27</sup>; however, a shorter TraR would not be expected to clash with i6. For the purpose of this analysis, we define two features of an “active” DksA: (1) a long CC domain and (2) a DxxDxA motif at the tip of an extended domain (CC in DksA and DksA2 or a single helix in TraR; Fig. 5). Substitutions in this motif compromise function of DksA<sup>18</sup>, DksA2 (RF et al., in preparation), and TraR<sup>1</sup>. Interestingly, although the first Asp residue is dispensable for *E. coli* DksA function<sup>18</sup>, this residue is highly conserved in the DxxDxA motif.

We reconstructed an approximate maximum likelihood phylogenetic tree of 965 DksA-like proteins that have an N-terminal extension using the FastTree program<sup>28</sup>. The intact DxxDxA motif was found in 677 sequences that we here tentatively define as functional

DksAs (Fig. 5b). 227 sequences contained a variation of this motif where the first Asp is replaced by His and/or Ala by Gly. While the wide distribution of this class suggests a potential function, it may be distinct from that of DksA where the Ala residue is critical for activity<sup>18</sup>.

Among 572 genomes, 230 have both functional DksA and i6, whereas 223 have neither. 119 genomes encode i6 but not DksA (Fig. 5c); in these bacteria, a non-homologous regulator may play a similar to DksA role. Thus, the distribution of DksA and i6 is strongly concordant: compared to the random expectation, the discordant patterns (DksA<sup>-</sup>i6<sup>+</sup> and DksA<sup>+</sup>i6<sup>-</sup>) are underrepresented by a factor of 2.5 ( $\chi^2$  test p-value of  $8 \times 10^{-54}$ ). Most strikingly, not a single genome has DksA unaccompanied by i6.

If the only role of i6 were to control access of DksA into the SC, the deletion of *dksA* could suppress the overexpression toxicity of i6 RNAP in *E. coli*. However, since removal of i6 compromises binding of GreA and GreB to RNAP, and *greA dksA*<sup>29</sup> and *greA greB dksA*<sup>9</sup> strains exhibit severe growth defects, we would expect to see a phenotype that resembles the *greA greB dksA* mutant upon deleting *dksA* in the i6 RNAP background. Indeed, we found that deletion of *dksA* in two different strain backgrounds exacerbated inhibitory effects of i6 RNAP (IA, unpublished data). We reason that an intricate interplay between different SC binding proteins in the cell<sup>9; 29</sup> precludes straightforward analysis of the DksA effect on i6 toxicity *in vivo*.

## Discussion

Here, we show that although DksA and GreB compete for binding to free RNAP, they do not interfere with each other's activities during elongation. We suggest that these and other SC factors bind to different conformations of the EC, which are in turn dictated by TL and adjacent  $\beta'$  domains. Most importantly, we show that the i6 insertion in the  $\beta'$  subunit controls DksA binding to the EC.

### Balanced action of the SC regulators

To maintain proper control of gene expression, the cell must keep a balance among all, known and putative, SC regulators. Synthesis of some of these proteins may be triggered in response to a particular signal, such as zinc limitation<sup>27</sup>. However, *E. coli* GreA, GreB and DksA are present at constant levels throughout the cell cycle<sup>9</sup>, in part due to feedback inhibition<sup>29; 30</sup> of their promoters, and an artificial increase in levels of one protein leads to pleiotropic effects on expression of many genes<sup>29; 31</sup>. While some of these changes are consistent with similar effects of all three factors on gene expression, others are not. Many of these overexpression phenotypes are not altered by substitutions of the "catalytic" acidic residues in GreA and DksA<sup>29</sup>, suggesting that they are due to competition for RNAP rather than to modification of transcription complexes. *In vitro* studies also paint a complex picture of similar and different effects on transcription. It is currently unknown which *in vivo* effects are direct and at what step of the transcription cycle they are exerted. We argue that RNAP controls which SC regulator binds to it depending on the context, directly affecting competition among them.

## Direct and indirect control by i6 and TL

The available data support a model in which the TL/i6 module plays a key role in regulation through the SC. Removal of the *E. coli* i6 inhibits activity of GreB<sup>14</sup> but increases activity of DksA during elongation<sup>8</sup>. These effects may be direct, mediated by (favorable or unfavorable) interactions between the i6 domain and the regulator, or indirect, mediated by conformational changes in TL. Zenkin and colleagues showed that TL is dispensable for the action of *T. aquaticus* Gre and proposed that Gre factors take place of TL in backtracked ECs, thereby enacting a switch from polymerization to nuclease activity<sup>7</sup>. i6 could mediate Gre activity indirectly, by influencing TL movement out of the SC; a putative change in TL is consistent with observations that i6 RNAP is resistant to pausing<sup>24</sup>, which is accompanied by TL misfolding<sup>32</sup>.

In the case of DksA, the main effect of i6 is likely direct - our modeling suggests that i6 hinders the entry of the CC domain into the SC (Fig. 3). Consistently, removal of i6 enhances DksA effects on elongation<sup>8</sup> and binding to ECs (Fig. 4). Small deletions in i6 (1045–1053 and 1040–1048::I) that should not eliminate a hypothetical clash with DksA had no effect on destabilization of promoter complexes by DksA, but conferred strong defects in pausing, and thus presumably altered TL in a similar way<sup>33</sup>, arguing against the indirect, TL-mediated effect of i6 on DksA activity. Nevertheless, we cannot exclude a possibility that removal of i6 also favors DksA activity by altering TL conformation. DksA effects on initiation are mediated in part through TL<sup>34</sup> and while completely folded TL is likely incompatible with DksA binding (OT, unpublished observations), it is possible that DksA and TL may undergo concerted changes in the SC. A putative interaction with DksA may “trap” a particular TL state, a common mechanism of bacterial RNAP inhibitors<sup>35;36</sup>. For example, DksA may act similarly to tagetitoxin, which we hypothesized stabilizes a folded state of TL<sup>35</sup>; consistently, tagetitoxin and DksA/ppGpp are competitive<sup>37</sup> and a R933A substitution in TL confers resistance to both tagetitoxin<sup>35</sup> and DksA (Supplementary Fig. 6). In contrast to tagetitoxin, the tip of DksA CC could be mobile (Fig. 3) and may undergo induced-fit changes upon binding to TL to establish productive interactions. We note, however, that TL is not required for DksA binding to RNAP<sup>8</sup>.

In summary, although GreB and DksA share the binding site on RNAP and some effects on transcription (Fig. 6), they differ dramatically in interactions with TL and i6. Gre proteins compete with TL, and their entry into the SC necessitates TL displacement, which occurs upon backtracking<sup>7</sup>. Although our data suggest that *E. coli* GreB may bind to i6 in these complexes, these interactions are not universally conserved but rather are a result of co-evolution in those species that have i6. In contrast, DksA likely establishes a functional contact with TL<sup>34</sup> and its binding to EC is hindered by i6. Differential contacts with i6 likely ensure that DksA, which outnumbers GreB 10:1 in the cell<sup>9</sup>, does not exclude GreB from arrested complexes: DksA affinity for backtracked ECs is more than 20 times lower than to core RNAP (Fig. 4c) whereas GreB binds backtracked ECs as tightly (Supplementary Fig. 3c) as the core enzyme<sup>38</sup>.



## What transcription complexes does DksA target?

We hypothesize that i6 serves as a sensor of RNAP state, thereby directing GreB and DksA action to a subset of transcription complexes. i6 is thought to move when TL unfolds<sup>19</sup>, e.g., during backtracking; this movement may favor i6/GreB interactions or facilitate GreB entry into the SC, explaining why GreB binds to WT EC-2 ~10-fold better than to complexes lacking i6 (Supplementary Fig. 3). In contrast, while DksA binds to ECs with at least 14-fold lower affinity than to the core enzyme when i6 is present, this difference is reduced to ~2.5 fold when i6 is deleted (Fig. 4). We suggest that i6 mobility may explain these differences: in EC (and RPo, which also binds to DksA poorly<sup>20</sup>), position of the jaw, which makes extensive contacts with i6, is constrained by the duplex DNA downstream from the active site, whereas in the core enzyme both i6 and jaw can be mobile. However, *in vitro*<sup>8</sup> and *in vivo*<sup>11</sup> data show that DksA is able to act during elongation by WT RNAP. What makes an EC a target for DksA?

We propose that weakened RNAP interactions with the downstream DNA may trigger the i6 release, allowing for DksA binding. At *rnmB* P1, DksA acts upon a promoter complex intermediate in which these contacts are not yet established, but not on RPo<sup>34</sup>. During elongation, RNAP contacts with the downstream DNA may be altered by the presence of a roadblock or a lesion; however, our observations that DksA alters elongation *in vitro* in the absence of roadblocks<sup>8</sup> suggest that DksA may bind to a transient intermediate in which i6 is repositioned, perhaps due to changes in TL. The effect of DksA on termination suggests that these interactions may also be altered when RNAP encounters a terminator.

## Methods

### Reagents

Oligonucleotides were obtained from Integrated DNA Technologies (Coralville, IA), NTPs – from GE Healthcare (Piscataway, NJ), <sup>32</sup>P-NTPs – from Perkin Elmer (Waltham, MA), restriction and modification enzymes – from NEB (Ipswich, MA), PCR reagents – from Roche (Indianapolis, IN), other chemicals – from Sigma (St. Louis, MO) and Fisher (Pittsburgh, PA). Plasmid DNAs and PCR products were purified using spin kits from Qiagen (Valencia, CA) and Promega (Madison, WI). All plasmids are listed in Table 1.

### Proteins

DksA<sup>4</sup>, GreB, and RNAP<sup>5</sup> were purified as described previously. DksA<sup>A35C</sup> was labeled with Atto 488 maleimide (Sigma); an excess dye was removed using G50 columns (GE Health). Labeling efficiency ranged between 60 and 100%. HMK-tagged DksA and GreB were labeled with <sup>32</sup>P-[ $\gamma$ ATP] using cyclic AMP protein kinase as described in<sup>5</sup>.

### Termination assays

Templates for *in vitro* transcription were generated by PCR amplification. Halted C105 ECs were formed in TGA14 (20 mM Tris-acetate, 20 mM Na acetate, 14 mM Mg acetate, 14 mM 2-mercaptoethanol, 0.1 mM EDTA, 5% glycerol, pH 7.9) with the starting substrates (150  $\mu$ M ApU, 5  $\mu$ M ATP and GTP, 2  $\mu$ M CTP, 2  $\mu$ Ci of <sup>32</sup>P-[ $\alpha$ CTP]; 3000 Ci/mmol) during 15 min incubation at 37 °C. Elongation was restarted by the addition of NTPs (to 250  $\mu$ M)

and heparin (to 10  $\mu\text{g/ml}$ ). The reactions were incubated for 10 min at 37 °C and quenched by addition of an equal volume of STOP buffer (10 M urea, 50 mM EDTA, 45 mM Tris-borate; pH 8.3, 0.1% bromophenol blue, 0.1% xylene cyanol).

### RNA cleavage assays

Halted complexes (A26) were prepared on pIA226 template in TGA2 buffer (same as TGA14 above but with 2 mM  $\text{Mg}^{2+}$  to minimize intrinsic cleavage) supplemented with ApU at 150  $\mu\text{M}$ , ATP and UTP at 2.5  $\mu\text{M}$ , GTP at 1  $\mu\text{M}$ , and 5  $\mu\text{Ci}$  of  $^{32}\text{P}$  [ $\alpha\text{GTP}$ ] (3000 Ci/mmol) during 15 min incubation at 37 °C and purified through G50 spin columns (GE Health). DksA (or storage buffer) was added followed by 3 min incubation at 37 °C. Cleavage reactions were initiated by the addition of GreB and quenched at selected times.

### Sample analysis

Samples were heated for 2 min at 90 °C and loaded on denaturing acrylamide (19:1) gels (7 M Urea, 0.5X TBE). RNA products were visualized and quantified using a PhosphorImager Storm 820 System (GE Healthcare), ImageQuant Software, and Microsoft Excel.

### Binding assays

Fe cleavage assays were performed as described in <sup>20</sup> using Atto 488-labeled DksA<sup>A35C</sup>,  $^{32}\text{P}$ [ $\gamma\text{ATP}$ ]-labeled HMK-DksA or HMK-GreB. See Supplementary Fig. 1 for additional details. Active EC0 and backtracked EC-2 complexes were assembled on oligonucleotide scaffolds (see Supplementary Table 1) at a 2:1 ratio of scaffold to RNAP to minimize the fraction of free RNAP. ECs were tested for nucleotide addition and Gre cleavage to ascertain the correct assembly. Activity assays and cleavage assays indicate that under these conditions core RNAP is completely bound to the scaffold. Titrations were done using increasing concentrations of ECs or free RNAP, with 10 nM DksA for ECs and 1 nM for RNAP (or 1 nM  $^{32}\text{P}$ [ $\gamma\text{ATP}$ ]-labeled GreB). Gels were analyzed using Typhoon 900 (GE Healthcare); see also Supplementary Data. An apparent  $K_d$  was calculated using the Scientist software (MicroMath) from at least three independent experiments.

### Competition assays

100 nM of fluorescently labeled DksA was incubated with RNAP and 2  $\mu\text{M}$  of a competitor protein for 15 minutes at 30°C. Fe-mediated cleavage was induced as described in <sup>20</sup>. Details are provided in the figure legends.

### Construction of the DksA/EC model

In building of the complex, DksA and the EC model were treated as rigid bodies. DksA CC was initially positioned on the enzyme similarly to GreB, for which a low-resolution EM model <sup>16</sup> and a large body of biochemical data <sup>3; 5; 15</sup> are available. Partially overlapping effects of GreB and DksA <sup>9; 18</sup> argue that this approach is justified. The position and orientation of DksA were then adjusted to avoid steric clashes and satisfy several experimental observations, as follows. First, the DksA CC tip is located within 10 Å of the active site  $\text{Mg}^{2+}$  ion, consistent with the observed cleavage by  $\bullet\text{OH}$  radicals generated in the active site (Fig. 1b). With its tip fixed, the orientation of the DksA CC still needed to be

determined. Steric constraints of the SC leave two rotational degrees of freedom, one in the plane parallel to RH and another around the axis along the helices of the CC domain. These rotations were determined, respectively, from two observations: (i) The RH tip interacts with DksA, explaining effects of Leu672/Val673 substitutions for Ala, Arg or Asp on DksA activity and binding<sup>8</sup>. In order to satisfy this observation, the C-terminal helix of DksA needed to be brought into contact with RH by a minor rotation of DksA. RH tip substitutions for Ala abolished DksA<sup>8</sup> but not GreB<sup>5</sup> function, indicating that these substitutions do not alter the RH structure. Indeed, while the RH structure is conserved, its sequence, including the tip residues, is variable. (ii) DksA Asn88 faces RH, consistent with an increase of DksA affinity for RNAP as a result of an Asn88 substitution for Ile<sup>13</sup>.

## Supplementary Material

Refer to Web version on PubMed Central for supplementary material.

## Acknowledgments

We thank Seth Darst for providing a model of *E. coli* GreB bound to EC and Georgy Belogurov and the members of the Gourse laboratory for stimulating discussions. This work was supported by the National Science Foundation (MCB-0949569; IA) and by the Intramural Research Program of the National Library of Medicine at National Institutes of Health (YIW).

## Abbreviations

<b>CC</b>	coiled-coil domain
<b>EC</b>	elongation complex
<b>RNAP</b>	RNA polymerase
<b>SC</b>	secondary channel
<b>TL</b>	trigger loop

## References

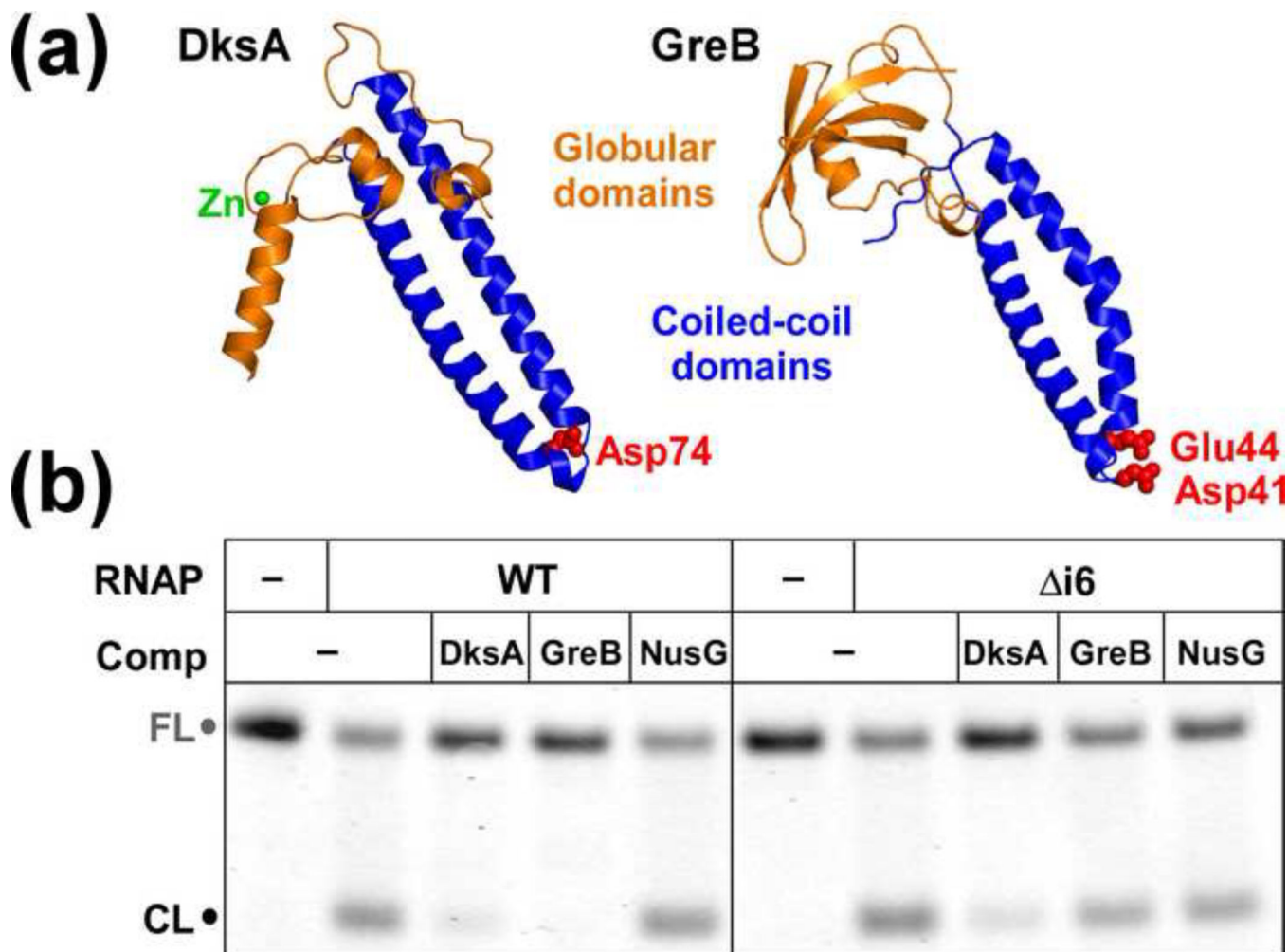
1. Blankschien MD, Potrykus K, Grace E, Choudhary A, Vinella D, Cashel M, Herman C. TraR, a homolog of a RNAP secondary channel interactor, modulates transcription. *PLoS Genet.* 2009; 5:e1000345. [PubMed: 19148274]
2. Lamour V, Rutherford ST, Kuznedelov K, Ramagopal UA, Gourse RL, Severinov K, Darst SA. Crystal structure of Escherichia coli Rnk, a new RNA polymerase-interacting protein. *J Mol Biol.* 2008; 383:367–79. [PubMed: 18760284]
3. Laptenko O, Lee J, Lomakin I, Borukhov S. Transcript cleavage factors GreA and GreB act as transient catalytic components of RNA polymerase. *EMBO J.* 2003; 22:6322–34. [PubMed: 14633991]
4. Perederina A, Svetlov V, Vassilyeva MN, Tahirov TH, Yokoyama S, Artsimovitch I, Vassilyev DG. Regulation through the secondary channel--structural framework for ppGpp-DksA synergism during transcription. *Cell.* 2004; 118:297–309. [PubMed: 15294156]
5. Vassilyeva MN, Svetlov V, Dearborn AD, Klyuyev S, Artsimovitch I, Vassilyev DG. The carboxy-terminal coiled-coil of the RNA polymerase beta'-subunit is the main binding site for Gre factors. *EMBO Rep.* 2007; 8:1038–43. [PubMed: 17917675]

6. Haugen SP, Ross W, Gourse RL. Advances in bacterial promoter recognition and its control by factors that do not bind DNA. *Nat Rev Microbiol.* 2008; 6:507–19. [PubMed: 18521075]
7. Roghanian M, Yuzenkova Y, Zenkin N. Controlled interplay between trigger loop and Gre factor in the RNA polymerase active centre. *Nucleic Acids Res.* 2011; 39:4352–9. [PubMed: 21266474]
8. Furman R, Sevostyanova A, Artsimovitch I. Transcription initiation factor DksA has diverse effects on RNA chain elongation. *Nucleic Acids Res.* 2012; 40:3392–402. [PubMed: 22210857]
9. Rutherford ST, Lemke JJ, Vrentas CE, Gaal T, Ross W, Gourse RL. Effects of DksA, GreA, and GreB on transcription initiation: insights into the mechanisms of factors that bind in the secondary channel of RNA polymerase. *J Mol Biol.* 2007; 366:1243–57. [PubMed: 17207814]
10. Dutta D, Shatalin K, Epshtein V, Gottesman ME, Nudler E. Linking RNA polymerase backtracking to genome instability in *E. coli*. *Cell.* 2011; 146:533–43. [PubMed: 21854980]
11. Tehranchi AK, Blankschien MD, Zhang Y, Halliday JA, Srivatsan A, Peng J, Herman C, Wang JD. The transcription factor DksA prevents conflicts between DNA replication and transcription machinery. *Cell.* 2010; 141:595–605. [PubMed: 20478253]
12. Trautinger BW, Jaktaji RP, Rusakova E, Lloyd RG. RNA polymerase modulators and DNA repair activities resolve conflicts between DNA replication and transcription. *Mol Cell.* 2005; 19:247–58. [PubMed: 16039593]
13. Blankschien MD, Lee JH, Grace ED, Lennon CW, Halliday JA, Ross W, Gourse RL, Herman C. Super DksAs: substitutions in DksA enhancing its effects on transcription initiation. *EMBO J.* 2009; 28:1720–31. [PubMed: 19424178]
14. Zhang J, Palangat M, Landick R. Role of the RNA polymerase trigger loop in catalysis and pausing. *Nat Struct Mol Biol.* 2009; 17:99–104. [PubMed: 19966797]
15. Loizos N, Darst SA. Mapping interactions of *Escherichia coli* GreB with RNA polymerase and ternary elongation complexes. *J Biol Chem.* 1999; 274:23378–86. [PubMed: 10438515]
16. Opalka N, Chlenov M, Chacon P, Rice WJ, Wriggers W, Darst SA. Structure and function of the transcription elongation factor GreB bound to bacterial RNA polymerase. *Cell.* 2003; 114:335–45. [PubMed: 12914698]
17. Tagami S, Sekine S, Kumarevel T, Hino N, Murayama Y, Kamegamori S, Yamamoto M, Sakamoto K, Yokoyama S. Crystal structure of bacterial RNA polymerase bound with a transcription inhibitor protein. *Nature.* 2010; 468:978–82. [PubMed: 21124318]
18. Lee JH, Lennon CW, Ross W, Gourse RL. Role of the coiled-coil tip of *Escherichia coli* DksA in promoter control. *J Mol Biol.* 2012; 416:503–17. [PubMed: 22200485]
19. Opalka N, Brown J, Lane WJ, Twist KA, Landick R, Asturias FJ, Darst SA. Complete structural model of *Escherichia coli* RNA polymerase from a hybrid approach. *PLoS Biol.* 2010; 8.
20. Lennon CW, Gaal T, Ross W, Gourse RL. *Escherichia coli* DksA binds to Free RNA polymerase with higher affinity than to RNA polymerase in an open complex. *J Bacteriol.* 2009; 191:5854–8. [PubMed: 19617357]
21. Lennon CW, Ross W, Martin-Tumas S, Touloukhonov I, Vrentas CE, Rutherford ST, Lee J-H, Butcher SE, Gourse RL. Direct interactions between the coiled-coil tip of DksA and the trigger loop of RNA polymerase mediate transcriptional regulation. *Genes Dev.* 2012 **in press**.
22. Ruan W, Lehmann E, Thomm M, Kostrewa D, Cramer P. Evolution of two modes of intrinsic RNA polymerase transcript cleavage. *J Biol Chem.* 2011; 286:18701–7. [PubMed: 21454497]
23. James E, Liu M, Sheppard C, Mekler V, Camara B, Liu B, Simpson P, Cota E, Severinov K, Matthews S, Wigneshweraraj S. Structural and Mechanistic Basis for the Inhibition of *Escherichia coli* RNA Polymerase by T7 Gp2. *Molecular cell.* 2012; 47:755–66. [PubMed: 22819324]
24. Artsimovitch I, Svetlov V, Murakami KS, Landick R. Co-overexpression of *Escherichia coli* RNA polymerase subunits allows isolation and analysis of mutant enzymes lacking lineage-specific sequence insertions. *J Biol Chem.* 2003; 278:12344–55. [PubMed: 12511572]
25. Ederth J, Artsimovitch I, Isaksson LA, Landick R. The downstream DNA jaw of bacterial RNA polymerase facilitates both transcriptional initiation and pausing. *J Biol Chem.* 2002; 277:37456–63. [PubMed: 12147705]
26. Tatusov RL, Fedorova ND, Jackson JD, Jacobs AR, Kiryutin B, Koonin EV, Krylov DM, Mazumder R, Mekhedov SL, Nikolskaya AN, Rao BS, Smirnov S, Sverdlov AV, Vasudevan S,

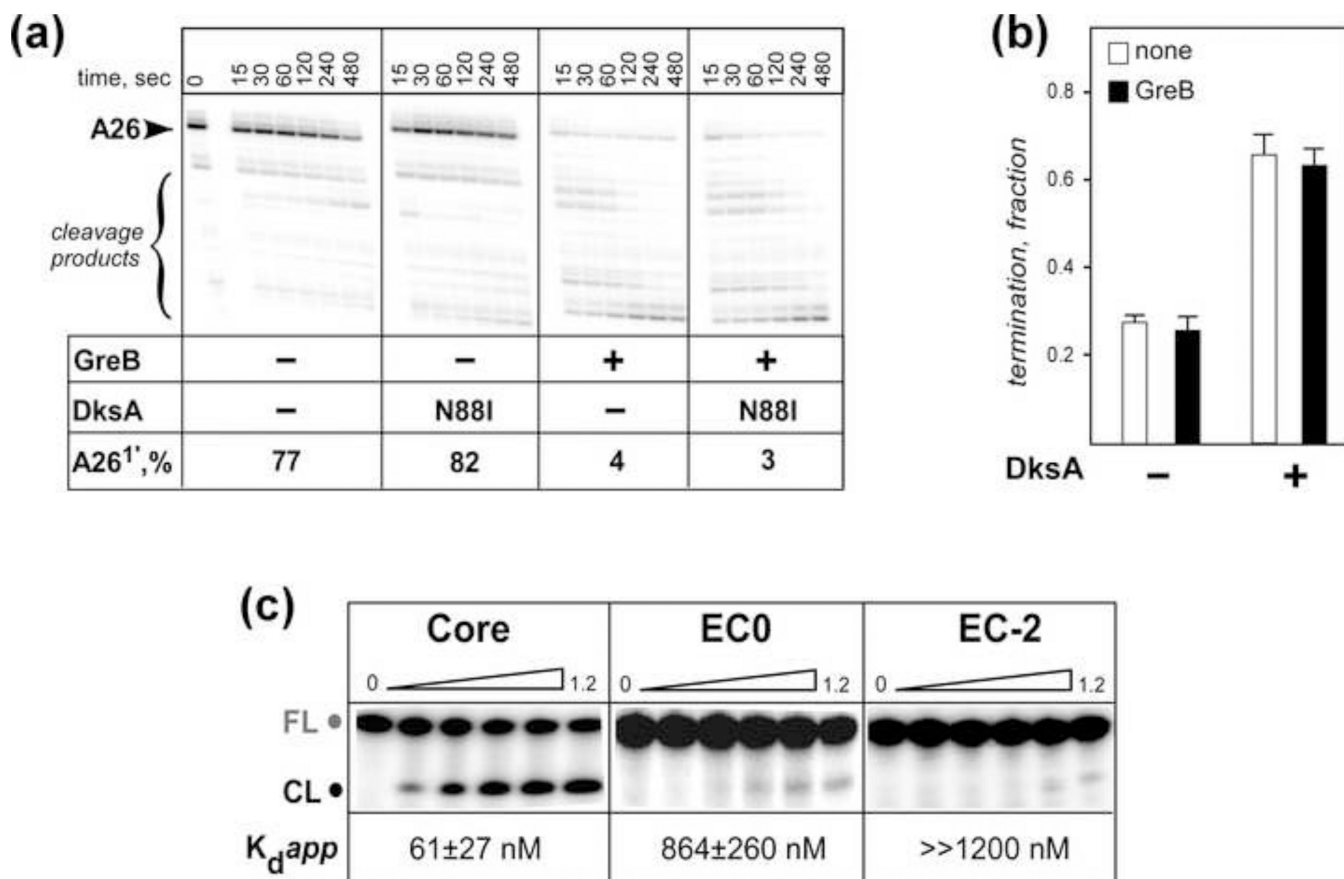
- Wolf YI, Yin JJ, Natale DA. The COG database: an updated version includes eukaryotes. *BMC bioinformatics*. 2003; 4:41. [PubMed: 12969510]
27. Blaby-Haas CE, Furman R, Rodionov DA, Artsimovitch I, de Crecy-Lagard V. Role of a Zn-independent DksA in Zn homeostasis and stringent response. *Mol Microbiol*. 2011; 79:700–15. [PubMed: 21255113]
  28. Price MN, Dehal PS, Arkin AP. FastTree: computing large minimum evolution trees with profiles instead of a distance matrix. *Mol Biol Evol*. 2009; 26:1641–50. [PubMed: 19377059]
  29. Vinella D, Potrykus K, Murphy H, Cashel M. Effects on growth by changes of the balance between GreA, GreB, and DksA suggest mutual competition and functional redundancy in *Escherichia coli*. *J Bacteriol*. 2012; 194:261–73. [PubMed: 22056927]
  30. Chandrangu P, Lemke JJ, Gourse RL. The dksA promoter is negatively feedback regulated by DksA and ppGpp. *Mol Microbiol*. 2011; 80:1337–48. [PubMed: 21496125]
  31. Aberg A, Shingler V, Balsalobre C. Regulation of the fimB promoter: a case of differential regulation by ppGpp and DksA in vivo. *Mol Microbiol*. 2008; 67:1223–41. [PubMed: 18284577]
  32. Toulkhonov I, Zhang J, Palangat M, Landick R. A central role of the RNA polymerase trigger loop in active-site rearrangement during transcriptional pausing. *Mol Cell*. 2007; 27:406–19. [PubMed: 17679091]
  33. Conrad TM, Frazier M, Joyce AR, Cho BK, Knight EM, Lewis NE, Landick R, Palsson BO. RNA polymerase mutants found through adaptive evolution reprogram *Escherichia coli* for optimal growth in minimal media. *Proc Natl Acad Sci U S A*. 2010; 107:20500–5. [PubMed: 21057108]
  34. Rutherford ST, Villers CL, Lee JH, Ross W, Gourse RL. Allosteric control of *Escherichia coli* rRNA promoter complexes by DksA. *Genes Dev*. 2009; 23:236–48. [PubMed: 19171784]
  35. Artsimovitch I, Svetlov V, Nemetski SM, Epshtein V, Cardozo T, Nudler E. Tagetitoxin Inhibits RNA Polymerase through Trapping of the Trigger Loop. *J Biol Chem*. 2011; 286:40395–400. [PubMed: 21976682]
  36. Vassilyev DG, Vassilyeva MN, Zhang J, Palangat M, Artsimovitch I, Landick R. Structural basis for substrate loading in bacterial RNA polymerase. *Nature*. 2007; 448:163–8. [PubMed: 17581591]
  37. Vassilyev DG, Svetlov V, Vassilyeva MN, Perederina A, Igarashi N, Matsugaki N, Wakatsuki S, Artsimovitch I. Structural basis for transcription inhibition by tagetitoxin. *Nat Struct Mol Biol*. 2005; 12:1086–93. [PubMed: 16273103]
  38. Laptenko O, Borukhov S. Biochemical assays of Gre factors of *Thermus thermophilus*. *Methods Enzymol*. 2003; 371:219–32. [PubMed: 14712703]
  39. Artsimovitch I, Svetlov V, Anthony L, Burgess RR, Landick R. RNA polymerases from *Bacillus subtilis* and *Escherichia coli* differ in recognition of regulatory signals in vitro. *J Bacteriol*. 2000; 182:6027–35. [PubMed: 11029421]
  40. Artsimovitch I, Landick R. Pausing by bacterial RNA polymerase is mediated by mechanistically distinct classes of signals. *Proc Natl Acad Sci U S A*. 2000; 97:7090–7095. [PubMed: 10860976]
  41. Belogurov GA, Vassilyeva MN, Svetlov V, Klyuyev S, Grishin NV, Vassilyev DG, Artsimovitch I. Structural basis for converting a general transcription factor into an operon-specific virulence regulator. *Mol Cell*. 2007; 26:117–29. [PubMed: 17434131]
  42. Svetlov V, Belogurov GA, Shabrova E, Vassilyev DG, Artsimovitch I. Allosteric control of the RNA polymerase by the elongation factor RfaH. *Nucleic Acids Res*. 2007; 35:5694–705. [PubMed: 17711918]

**Highlights**

- DksA and GreB bind to the same site on free RNA polymerase.
- DksA does not bind to elongation complexes and cannot compete with GreB.
- The i6 domain prevents DksA binding to transcription complexes.
- All bacterial genomes that have DksA also have i6.
- DksA may target transcription complexes in which i6 becomes mobile.



**Fig. 1.** DksA and GreB share a similar structural organization and compete for binding to RNAP. (a) Structures of *E. coli* DksA<sup>4</sup> and GreB<sup>5</sup>. Both proteins contain functionally critical acidic residues (indicated by red spheres) at the tips of their CC domains. A zinc atom bound to the Cys4 Zn-finger in DksA is shown as a green sphere. (b) Competition between fluorescently labeled DksA<sup>A35C</sup> (100 nM) and unlabeled factors (Comp, 2  $\mu$ M) for binding to core RNAPs (400 nM) by Fe-mediated cleavage; FL - full length DksA, CL - cleaved DksA.

**Fig. 2.**

DksA and GreB target different ECs. (a) Transcript cleavage assays. Halted  $^{32}\text{P}$ -[ $\alpha\text{GTP}$ ] labeled A26 ECs were formed on pIA226 template. DksA<sup>N88I</sup> was added at 10  $\mu\text{M}$  where indicated. Cleavage reactions were started by addition of GreB (to 100 nM); aliquots were quenched at the indicated times. The fraction of uncleaved A26 RNA after 1 min incubation is shown below the gel. The assay was repeated at least three times for each combination of factors; the differences between independent measurements were within 10%. (b) Termination assays were carried out on pIA1088 (*trnB* T1) template with 2  $\mu\text{M}$  DksA<sup>N88I</sup> and 20  $\mu\text{M}$  GreB. The data represent the average  $\pm$  standard deviation for three independent experiments. (c) DksA binds poorly to active (EC0) and backtracked (EC-2) complexes assembled on scaffolds;  $^{32}\text{P}$  [ $\gamma\text{ATP}$ ] -labeled DksA (at 10 nM) was incubated with increasing concentrations RNAP or EC (up to 1.2  $\mu\text{M}$ ) for 15 minutes at 37°C. Following Fe-mediated cleavage for 15 minutes at 37°C, the reactions were analyzed on denaturing SDS gels.



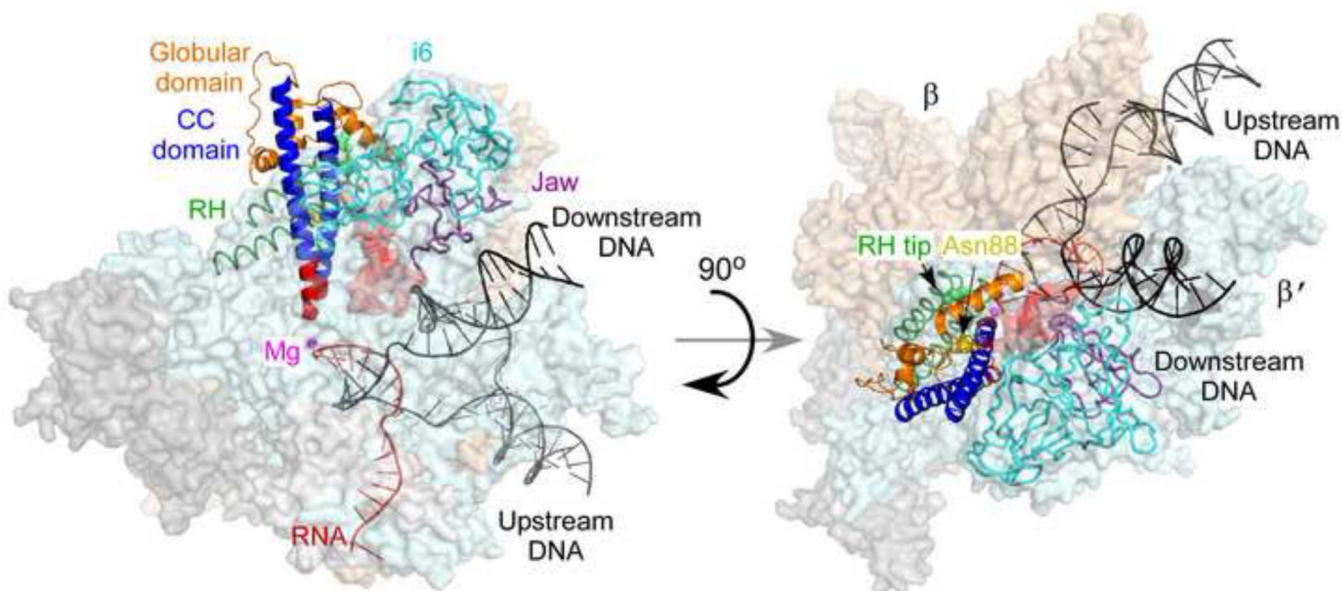


**Fig. 3.** The  $\beta'$  i6 domain controls DksA access into the SC. A model of DksA bound to *E. coli* EC. RNAP is shown as transparent surface,  $\beta'$  is in light cyan,  $\beta$  – in wheat,  $\alpha$  and  $\omega$  – in grey. DNA is in black and RNA – in red. The active site Mg is shown as a magenta sphere. The  $\beta'$  regions discussed in the text, RH (green), jaw (dark purple), and i6 (cyan), are shown as strings. DksA is shown as a cartoon and colored as in Figure 1; Asn88 in DksA (yellow) and the RH tip residues (green) are shown as spheres. Two regions are colored red to indicate their conformational flexibility: (1) TL, which is known to change conformation during the nucleotide addition cycle and upon binding of inhibitors, and (2) the tip of DksA CC and its flanking helical regions that are flexible, as evidenced by our recent structural data (Furman et al., in preparation).

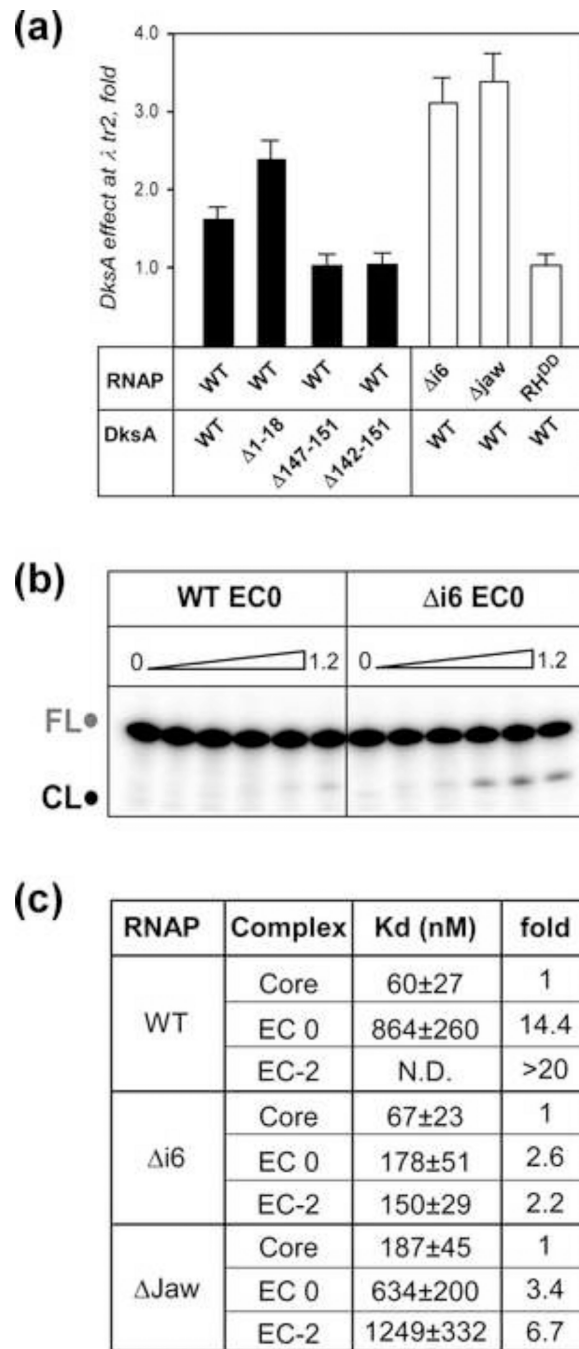


**Fig. 4.** Functional tests of the EC/DksA model. (a) DksA ability to stimulate termination at  $\lambda$ tr2 *in vitro* is altered by changes in RNAP and DksA. The data represent the average  $\pm$  standard deviation of three independent experiments. (b) Deletion of i6 facilitates DksA binding to EC.  $^{32}$ P[ $\gamma$ ATP]-labeled DksA (10 nM) was incubated with increasing concentrations of core, an active EC, or a backtracked EC formed with different RNAP variants. The cleaved fraction of DksA was plotted against RNAP concentration and the apparent affinity was calculated from an average ( $\pm$ standard deviation) of at least three independent repeats. The

maximum cleavage of DksA in the presence of EC was lower as compared to free RNAP (10% compared to 30% respectively). (c) The deletion of i6 and a partial deletion of the jaw domain increase the affinity of DksA to the EC. We could not determine the affinity of DksA to EC-2 in the concentrations range tested.

Author Manuscript

Author Manuscript

Author Manuscript

Author Manuscript

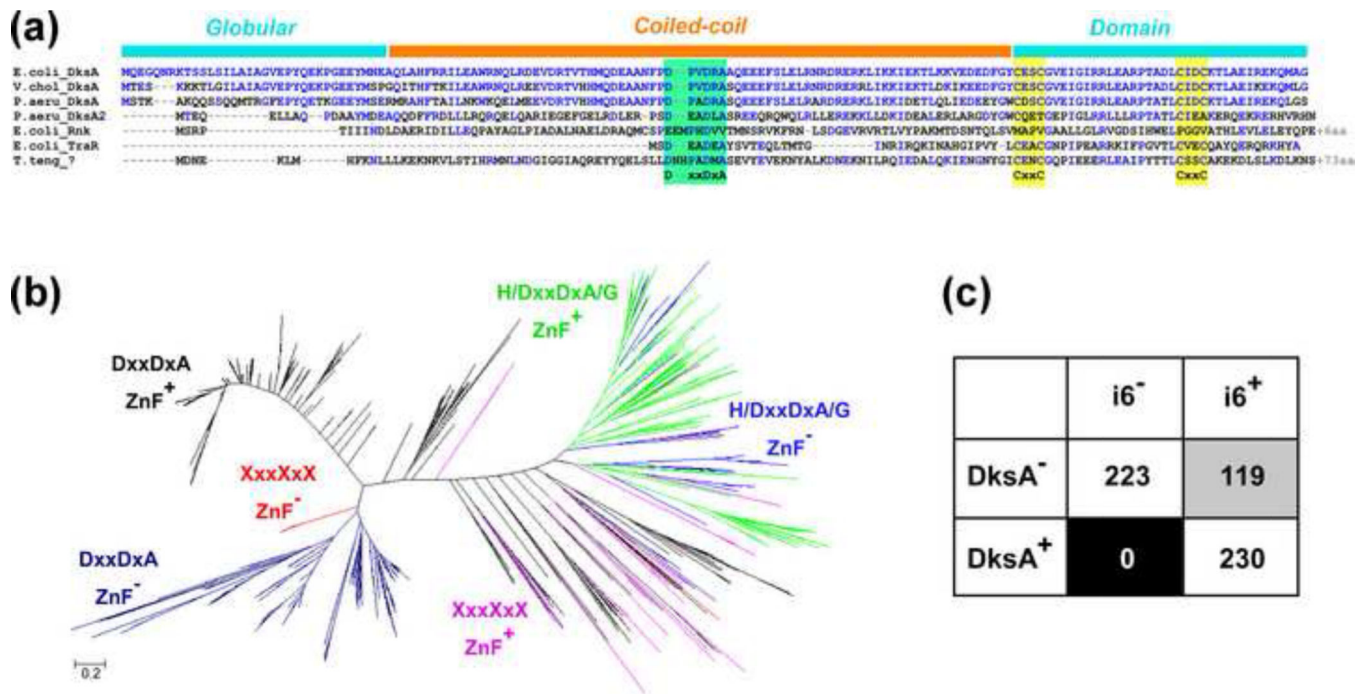


**Fig. 5.** Distribution of DksA and  $i6$  in bacterial genomes. (a) Alignment of the *E. coli* DksA, TraR and Rnk and DksA-like proteins from *Vibrio cholerae*, *P. aeruginosa*, and *Thermoanaerobacter tengcongensis*. The CC tip DxxDxA motif is highlighted in green, the Cys4 Zn finger - in yellow. (b) A phylogenetic tree of DksA-like proteins. Colors of the branches correspond to different COG1734 families: black, canonical Zn-finger DksAs; dark blue, DksA2-like proteins lacking the Zn-finger; green, Zn-finger proteins that contain (potentially inactivating) substitutions in the CC tip; blue, proteins that lack both the Zn-finger and a “functional” CC tip; magenta and red, variants with or without the Zn-finger, respectively, that lack the DxxDxA motif. (c) Distribution of DksA and  $i6$  in representative genomes.

	<b>Gre factors</b>	<b>DksA</b>
<b>Transcription initiation</b>	pleiotropic, partially overlapping promoter-dependent effects	
<b>Rescues stalled RNAP <i>in vivo</i></b>	<b>YES, presumably <i>via</i> RNA cleavage</b>	<b>YES, by unknown mechanism</b>
<b>Target EC</b>	<b>backtracked</b>	<b>unknown</b>
<b>RNA chain elongation</b>	<b>no effect</b>	<b>inhibits</b>
<b>RNA cleavage activity</b>	<b>stimulates</b>	<b>no effect</b>
<b>Rim helices domain</b>	serves as a major binding site	
<b>Trigger loop</b>	<b>dispensable</b>	<b>required, may interact</b>
<b>i6 domain</b>	<b>stimulates, may interact</b>	<b>inhibits</b>

**Fig. 6.** Similarities between DksA and GreB activities and interactions with RNAP domains. See text for detailed discussion and references.

Table 1

Plasmids.

Name	Description	Source/reference
pIA226	$\lambda$ P <sub>R</sub> promoter-A26- <i>hisP</i>	39
pIA247	P <sub>T7</sub> promoter - <i>nusC</i> <sup>His6</sup>	40
pIA536	<i>rrnB</i> P1 promoter	27
pIA576	P <sub>T7</sub> promoter -[HMK] <i>greB</i> <sup>His6</sup>	5
pIA578	P <sub>T7</sub> promoter - <i>greA</i> <sup>His6</sup>	This work
pIA579	P <sub>T7</sub> promoter - <sup>CBD</sup> [HMK] <i>dksA</i>	4
pIA680	P <sub>T7</sub> promoter - <sup>CBD</sup> <i>dksA</i> [ 147-151] <sup>I</sup>	This work
pIA681	P <sub>T7</sub> promoter - <sup>CBD</sup> <i>dksA</i> [ 142-151]	This work
pIA840	P <sub>T7</sub> promoter - <sup>CBD</sup> <i>dksA</i> [N88I]	8
pIA1024	P <sub>T7</sub> promoter- <i>rpoA-rpoB-rpoC</i> [ 1149-1190] <sup>His6</sup> - <i>rpoZ</i>	This work
pIA1047	P <sub>T7</sub> promoter- <sup>CBD</sup> <i>dksA</i> [A35C]	8
pIA1088	T7A1 promoter-C105- <i>rrnB</i> T1 terminator	8
pIA1116	T7A1 promoter-C105- $\lambda$ tr2 terminator	This work
pIA1152	P <sub>T7</sub> promoter - <sup>cbd</sup> <i>dksA</i> [ 1-18]	This work
pVS10	P <sub>T7</sub> promoter- <i>rpoA-rpoB-rpoC</i> <sup>His6</sup> - <i>rpoZ</i>	41
pVS11	P <sub>T7</sub> promoter - <sup>CBD</sup> <i>dksA</i>	4
pVS14	P <sub>T7</sub> promoter- <i>rpoA-rpoB-rpoC</i> [ 943-1130] <sup>His6</sup> - <i>rpoZ</i>	42
pVS50	P <sub>T7</sub> promoter- <i>rpoA-rpoB-rpoC</i> [672,673DD] <sup>His6</sup> - <i>rpoZ</i>	5

<sup>I</sup>CBD = Chitin-binding domain - intein fusion from pTYB12 (NEB); HMK = heart muscle kinase recognition motif, RRASV.